PHYSICAL REVIEW B

CONDENSED MATTER

THIRD SERIES, VOLUME 49, NUMBER 4 15 JANUARY 1994-II

Electron transport along a spatially disordered chain in the presence of dissipation

Klaus Maschke
Institut de Physique Appliquée, Ecole Polytechnique Fédérale, CH 1015 Lausanne, Switzerland

Michael Schreiber
Institut für Physikalische Chemie, Johannes-Gutenberg-Universität, D-55099 Mainz, Federal Republic of Germany
(Received 4 June 1993; revised manuscript received 20 September 1993)

The electronic dc transport along a spatially disordered chain of scatterers is described within the Landauer-Büttiker approach. The chain is composed of single scatterers which allow for elastic as well as for inelastic processes. The scattering matrix of the disordered chain is calculated with a recursive method. In the absence of dissipation the transmission coefficient and the dc conductance decrease exponentially with the length of the chain. We show that these disorder effects are gradually suppressed with increasing dissipation. For large dissipation the conductivity of the chain becomes even independent of the disorder. The results allow us to relate the onset of the dc conduction at finite temperature to the loss of phase memory during inelastic collisions of the electrons. Further we analyze the decrease of the chemical potential along the chain in presence of disorder. For small dissipation we find a strikingly nonuniform behavior, which is characterized by large steps and nearly constant plateaus in between.

I. INTRODUCTION

Since the pioneering work of Mott[1] and Landauer[2] it has been well established that for sufficiently low temperatures the dc electronic transport in disordered systems is determined by the localization properties of the electromic wave functions near the Fermi level E_F. For strongly localized states near E_F, i.e., small spatial overlap between the current carrying states, the electronic transport is generally described in terms of the hopping model,[1] which is based on the assumption that the hopping rate between localized states decreases exponentially with respect to the distance between the respective localization centers. The hopping picture breaks down in the limit of weak localization, where the spatial distance between the current carrying states near E_F is much smaller than the localization length. In this case it can be expected that interference effects become important. This situation can more adequately be described within the less restrictive approach of Landauer,[2] which expresses the dc conductance in terms of the scattering matrix of the sample. For vanishing dissipative scattering within the sample the dc conductance is determined by the transmission probability at E_F.[2]

The Landauer approach has proven to be very useful for analytical as well as numerical studies of nondissipative conduction in disordered systems. It has in particular been the motivation for the recursive calculations of the transfer matrices of quasi-one-dimensional systems in order to determine the Lyapunov exponents which characterize the exponential decay of the localized electronic wave functions.[3] In this picture the localization of the electronic states is understood as a consequence of the destructive interference between coherently multiply scattered waves in a disordered sample. Bearing in mind that phase coherence will be destroyed by dissipative processes, we obtain an alternative picture of the dc conduction in presence of localized states, namely that the onset of dc conduction at finite temperature should be related to the loss of phase memory. This idea, which is apparently rather different from the hopping model, will be pursued in the present work.

For this purpose, we calculate the dc conductance of a spatially disordered chain of single scatterers within the Landauer approach in presence of dissipative scattering processes.[4–6] A one-dimensional disordered system with elastic scattering only was numerically studied by Lenstra and Smokers,[7] who determined the average transmission probability and derived a Landauer-type expression for the resistance. The average resistivity of a disordered chain with inelastic scattering was calculated by Band *et al.*[8] in a semiempirical approach. The conductance of an ordered quantum wire has been discussed within a continuum approach for inelastic scattering.[9] D'Amato and Pastawski[10] have used the Landauer approach to determine the conductance of ordered and disordered chains in presence of inelastic scattering. How-

ever, whereas in their work the scattering probabilities are calculated with a Green's function mean field method, we propose here a rather different approach, which is based on the recent extension of the Landauer theory to ordered dissipative systems.[4–6] For disordered systems this method has already been shortly discussed in Ref. 11, where also preliminary results for the behavior of the transmission probability have been reported.

We consider a system composed of single scatterers which do not only allow for elastic scattering within the transport channels, but also provide scattering into side channels connected to an electron reservoir or heat bath where the electrons are thermalized.[4] This is not just a toy model but a reasonable description, e.g., for a polymer chain, in which the constituting monomers are represented by single scatterers and where the intramolecular vibrations as well as the vibrational modes of the environment (such as side chains or solvents, if they exist) provide the heat bath. In this picture the side channels of a single scatterer can be visualized as a side loop in which the electrons couple to a heat bath, i.e., a phonon reservoir. This approach allows us to study the effects of dissipation on the conductivity of polymer chains, and it shall be used in the future to extend existing studies[12,13] of disordered polyanilines. We note that a similar interpretation of the phase destroying side channels has been given by Datta,[14] who has introduced an ensemble of harmonic oscillators to describe the heat bath. In contrast, Büttiker[4] has connected the side channels to electron-rich reservoirs. Current conservation in the transport channels is imposed, so that no net current is allowed into or out of the reservoirs. Consequently, electrons entering the reservoirs lose their phase memory. In this way, for example, the transport of electrons through heterostructures can be modeled, alternating strongly scattering barriers and more or less incoherently transmitting layers. An interesting topic in this context is the spatial dependence of the chemical potential which can be "measured" by means of the side channels.[4,6] Provided that electron screening is efficient, the chemical potential reflects the voltage drop across the sample as discussed by Landauer.[15,16] In the following we shall usually refer to this interpretation of the model to visualize the consequences of our numerical results. Analogously, the relation between the local voltage and the change in the local electrochemical potential[17] was recently used to determine a local resistance in terms of an equilibrium resistor.[18]

To obtain our results, the transport properties of the full chain are expressed in terms of its scattering matrix, which can be calculated exactly using a recursive method.[11,19] First we investigate the decay behavior of the elastic transmission probability, which means the scattering probability directly between the incoming and the outgoing transport channel, disregarding the contribution of electrons entering and leaving the reservoirs. We further analyze the behavior of the chemical potential along the chain. This problem has been posted by Landauer[15] recently. We find that the usual assumption of a linear decrease of the chemical potential between the contacts is not valid for small dissipation. While it is not really surprising that the chemical potential changes in a nonuniform way across the sample, it may be quite striking to realize that for small dissipation its drop between the contacts is determined by very few large steps. This behavior is reminiscent of hopping transport along a disordered chain, which is governed by the segments of the chain with the lowest hopping probabilities. Based on this investigation, we finally discuss the behavior of the dc conductance in presence of disorder and dissipation.

Two different regimes have to be distinguished already in the ordered chain,[5] both corresponding to different ranges of wave vectors q: In the "surface regime" incoming waves can penetrate into the sample over a finite distance only; the elastic transmission probability vanishes exponentially with the chain length due to destructive interference of the multiply backscattered waves, and in this case dissipative scattering reduces the destructive interference and thus increases the (exponentially small) conductance. The situation is different in the "bulk regime," in which the incoming waves are coherently transmitted with finite probability for arbitrary length of the chain. It is shown below that in this regime, where the transmission coefficient of the ordered sample oscillates as a function of the chain length, both disorder and dissipation lead to an exponential decrease of the elastic transmission probability. Accordingly, the dc conductance of a disordered chain vanishes in the limit of small dissipation. With increasing dissipation the influence of disorder in the bulk regime is shown to be gradually suppressed. For large dissipation the conductance becomes completely independent of the disorder.

Using band structure terminology, the surface regime may be called a forbidden band, because incoming waves can penetrate the sample only over a finite length. In the band picture the introduction of disorder leads to a smearing out of the edges of the allowed bands. The appearing band tails contain strongly localized states, so that transport is enabled by disorder, although exponentially decreasing with increasing system size. In our scattering approach we find an analogous behavior near the edge of the bulk regime. Here the disorder leads to an increased elastic transmission probability in the surface regime. In order to avoid confusion we emphasize that in our picture the surface and bulk regimes comprise scattering states which are distinguished by their wave vector q, while in the usual band picture the forbidden and allowed bands correspond to different energy intervals. It should be noted, however, that for the chain of parametrized scatterers introduced below the wave vector q cannot be related to a respective energy, because we do not have a dispersion relation. The specific influence of the energy dispersion on the electron transport will be discussed in a future paper, where we relate the scattering parameters to the Anderson Hamiltonian.[20]

II. THEORETICAL APPROACH

Following Refs. 5, 6, and 11, we consider single scatterers, which allow for scattering between four channels as indicated in Fig. 1. The different scatterers will be linked

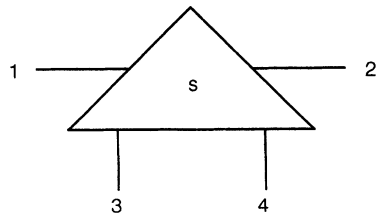

FIG. 1. Single scatterer. The channels 1 and 2 are the transport channels, channels 3 and 4 denote the heat bath channels.

via the transport channels 1 and 2. The side channels 3 and 4 connect the system to electron reservoirs or heat baths which are defined by their statistical properties and thus account for the inelastic scattering processes within the sample. Assuming the single scatterer to be positioned at the origin, the elastic scattering between the transport channels can be described by the 2×2 scattering matrix

$$\mathbf{s}_{\mathrm{el}} = \begin{pmatrix} r & t \\ t & r \end{pmatrix} \tag{1}$$

in the absence of dissipation. In the following we parametrize the reflection coefficient r and the transmission coefficient t in terms of the elastic transmission probability δ of the single scatterer:

$$\begin{aligned} r &= i\sqrt{1-\delta}, \\ t &= \sqrt{\delta} \qquad \text{with } 0 \le \delta \le 1. \end{aligned} \tag{2}$$

The single scatterers (see Fig. 1) are fully described by a 4×4 scattering matrix $\mathbf{s}$, which relates the incoming waves in all four channels to the corresponding outgoing waves. It can be written as

$$\mathbf{s} = \begin{pmatrix} \alpha & \mathbf{s}_{\mathrm{el}} & \beta & \mathbf{1} \\ \beta & \mathbf{1} & -\alpha & \mathbf{s}_{\mathrm{el}}^{*} \end{pmatrix} \tag{3}$$

in terms of the inelastic scattering probability ϵ:

$$\begin{aligned} \alpha &= \sqrt{1-\epsilon}, \\ \beta &= \sqrt{\epsilon} \qquad \text{for } 0 \le \epsilon \le 1. \end{aligned} \tag{4}$$

The 2×2 unity matrix $\mathbf{1}$ in Eq. (3) mediates the coupling between the transport channels and the heat bath channels. Thus $\epsilon = 0$ corresponds to a completely elastic scatterer which is decoupled from the heat bath and $\epsilon = 1$ means a completely inelastic scatterer by which the waves in the transport channels are entirely deviated into the heat bath. Other couplings between the transport channels and the side channels have been discussed by Burmeister *et al.*[19] The inclusion of the submatrix $-\mathbf{s}_{\mathrm{el}}^{*}$ ensures the unitarity of $\mathbf{s}$. It is worthwhile to note that this part of the scattering matrix does not influence the physical results and in particular that it does not enter the transport equations.[19]

We now consider a spatially disordered chain of N scatterers as sketched in Fig. 2. The individual scatterers are linked by the transport channels 1 and 2, and the remaining channels are used to connect each scatterer to its electron reservoir or heat bath. We assume that there is no correlation between the different reservoirs or heat baths. The positions of the single scatterers n $(1 \le n \le N)$ are given by

$$x_n = x_{n-1} + a(1 + r_n), \tag{5}$$

where the r_n are random numbers which are uniformly distributed over the interval $[-W/2, W/2]$, and where the average distance between the scatterers, i.e., the lattice constant in the ordered case, is given by a. The scattering of a plane wave which enters the system through one of the channels is described by the scattering matrix $\mathbf{S}^N$ of the entire chain. $\mathbf{S}^N$ can be calculated in an efficient manner with our recursive method, which has been introduced in Ref. 11 and analyzed in detail in Ref. 19. The spatial positions of the single scatterers enter the calculation of $\mathbf{S}^N$ via the phase factors

$$\varphi_{n-1,n}^{q} = e^{iq(x_n - x_{n-1})} = e^{iqa(1+r_n)}, \tag{6}$$

which describe the phase shifts between two successive scattering events at sites $n-1$ and n for a given wave vector q.

The scattering probabilities p_{ij} between channels i and j of the chain are obtained from $\mathbf{S}^N$ as

$$p_{ij} = \mid \mathbf{S}_{ij}^{N} \mid^2 . \tag{7}$$

In particular, p_{21} describes the elastic transmission probability between channels 1 and 2, i.e., directly through the entire chain without diversion into and out of any reservoir. This quantity completely determines the transport in absence of dissipation within the chain, and therefore it will be studied in detail in the present paper. In

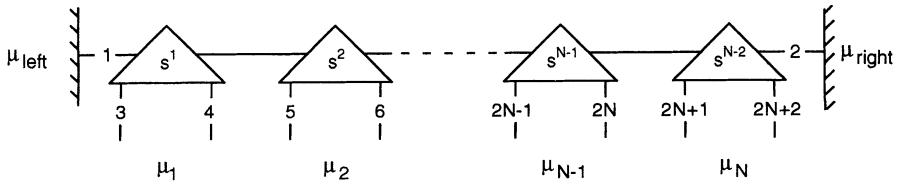

FIG. 2. Chain of N scatterers between two contacts with the corresponding chemical potentials μ_i for the ith scatterer and μ_{left} and μ_{right} for the contacts. The labeling of the channels corresponds to the scattering matrix of the chain.

the general case, it depends on the dissipation parameter ϵ and on the disorder parameter W, therefore we write $p_{21} = p_{21}(\epsilon, W)$. For the subsequent discussion we introduce the dissipation-induced decay length ζ by

$$p_{21}(\epsilon, 0) = p_{21}(0, 0) \exp(-N/\zeta) \tag{8}$$

and the disorder-induced decay length ξ by

$$p_{21}(\epsilon, W) = p_{21}(\epsilon, 0) \exp(-N/\xi). \tag{9}$$

Thus ζ describes the leakage through the side channels for the ordered chain, whereas ξ characterizes the influence of the disorder for a given dissipation parameter ϵ. It should be noted that it is *a priori* unclear whether definitions (8) and (9) are reasonable, i.e., whether the elastic transmission probability p_{21} decays exponentially, so that ζ and ξ become independent of the chain length for large N. We demonstrate below that this is indeed the case. The overall decay of the elastic transmission probability is then described by

$$p_{21}(\epsilon, W) = p_{21}(0, 0) \exp(-N/\lambda) \tag{10}$$

with the total decay length λ given by

$$\frac{1}{\lambda} = \frac{1}{\zeta} + \frac{1}{\xi}. \tag{11}$$

The second transport property which we will analyze in the present paper is the resistance or its inverse, the conductance. It depends not only on the elastic transmission probability p_{21}, but also on the scattering probabilities between the transport channels and the side channels. For the calculation of the resistance we consider the situation of Fig. 2, where contacts with different chemical potentials μ_{left} and μ_{right} are attached to the transport channels 1 and 2 of the chain of N scatterers. The chemical potentials $\mu(i)$, which are attributed to the different channels i, are the same for the two side channels of each individual scatterer (see Fig. 2), i.e., we have

$$\begin{aligned} \mu(1) &= \mu_{\text{left}}, \\ \mu(2) &= \mu_{\text{right}}, \\ \mu(2n+1) = \mu(2n+2) &= \mu_n \qquad \text{for } n=1,\ldots,N. \end{aligned} \tag{12}$$

The chemical potentials μ_n for $n = 1, \ldots, N$ are obtained from the current conservation conditions

$$I_n = I(2n+1) + I(2n+2) = 0, \tag{13}$$

where the currents are determined by (see, e.g., Ref. 5)

$$I(i) = \frac{e}{h} \sum_{j=1}^{2N+2} p_{ji}[\mu(i) - \mu(j)] \qquad \text{for } i = 1,\ldots,2N+2. \tag{14}$$

Following the arguments of Ref. 5, we obtain for the resistance of the chain, including the contact resistance,

$$R(N) = \frac{h}{e^2} \frac{1}{p_{21} + \sum_{n=1}^{N} \chi_n p_f(n)}, \tag{15}$$

where χ_n are the normalized chemical potentials

$$\chi_n = \frac{\mu_n - \mu_{\text{right}}}{\mu_{\text{left}} - \mu_{\text{right}}}, \tag{16}$$

which shall also be discussed in detail below. The forward scattering probabilities $p_f(n)$ in Eq. (15) describe the total scattering probability from the side channels of the scatterer n into the transport channel 2, i.e.,

$$p_f(n) = p_{2,2n+1} + p_{2,2n+2}, \tag{17}$$

where the scattering probabilities p_{ij} are given by Eq. (7).

For the discussion of our results it will be convenient to introduce the quantity

$$\sigma(N) = \frac{N}{R(N) - h/e^2}, \tag{18}$$

which defines the conductivity for sufficiently large N. The subtracted value h/e^2 in the denominator represents the contact resistance (see Ref. 5).

Recently there has been some discussion in the literature[15,21–24] whether it is necessary to take the Pauli exclusion principle into consideration in the determination of the current [Eq. (14)]. This would lead to a blocking factor $1 - f$ with an appropriate occupation probability f accounting for the other electrons already in the system. In the following we give a plausibility argument that the above derivation is consistent without additional blocking factors. First, we consider *two* reservoirs i and j. In this case, as mentioned by Landauer,[15] the respective additional terms cancel in the calculation of the net transition rate between the reservoirs, provided that the scattering probability is symmetric, i.e., $p_{ij} = p_{ji}$. In addition to that, the question arises[15,23,24] whether electrons emitted from *other reservoirs* could hinder the transmission in a particular channel. This is, however, impossible, since the different reservoirs have been assumed to be uncorrelated, and therefore electrons coming from different reservoirs are in *orthogonal states* as pointed out by Landauer,[15] too. These orthogonal states can be populated independently and therefore Pauli exclusion does not apply. In conclusion, there are no additional blocking factors required in our case because the symmetry of the individual scatterers leads to the symmetry of the total scattering matrix, so that the condition $p_{ij} = p_{ji}$ is fulfilled. The symmetric parametrization of the inelastic scattering (3) is the crucial point here. Datta[21] has shown that the condition of symmetric inelastic transmission is obeyed in the linear-response regime. The situation is different if the inelastic scattering probability depends on the energy of the incoming electron, which could be due, e.g., to a time-dependent potential[22,23] or to a specific microscopic description of the interaction between the electron and the inelastic scatterer.[24]

III. NUMERICAL RESULTS

A. Elastic transmission probability

In the following we discuss our results for $W = 1$, which corresponds to a relatively strong disorder. For small dissipation the electron transport across the chain is governed by the behavior of the elastic transmission probability p_{21} [see Eq. (15)]. The wave-vector dependence of p_{21} for the ordered and the disordered chain in absence of dissipation is shown in Fig. 3 for a relatively small sample of 20 scatterers. As already discussed in Ref. 5, the elastic transmission probability of the ordered chain is symmetric with respect to $\pi/2a$ and becomes very small near $q = 0$ and $q = \pi/a$. In these surface regimes incoming waves penetrate the chain over a finite distance only and p_{21} decreases exponentially with the length of the chain. This can be understood as a consequence of the destructive interference of multiply scattered waves. In this q range the elastic transmission probability p_{21} of the ordered chain is small already in the case of only 10 to 20 scattering sites, but for the subsequent discussion it should be noted that it does not completely vanish even for long chains. For intermediate q values we find a transmission window, which is characterized by $N - 1$ rapid oscillations of p_{21}. Already for rather short chains the amplitude of the oscillations as well as the width of the transmission window become practically independent of the length of the chains and depend only on the elastic transmission probability δ of the single scatterer in Eq. (2). In contrast to the surface regime we call this q range the bulk regime because the incoming waves are sustained in the bulk. The width of this transmission window increases with the parameter δ. At the same time, the envelope function which describes the minimum of the elastic transmission p_{21} in this regime (cf. Fig. 3) is lifted towards higher values, i.e., the amplitudes of the oscillations decrease with increasing δ. In the limit $\delta = 1$ no reflection takes place at the single scatterers [cf. Eq. (2)], and the waves are transmitted with probability 1 through the chain, for all q values and independent of the positions of the scatterers.

In the following we present characteristic results for $\delta = 0.7$. The results for other δ values are very similar, and the δ dependence can easily be understood from the above arguments. The range of the transmission window for $\delta = 0.7$ is given by $0.18\pi/a \leq q \leq 0.82\pi/a$ (see Fig. 3).

In Fig. 3 we have also displayed the behavior of the elastic transmission probability p_{21} in the presence of spatial disorder. In this case the symmetry with respect to $q = \pi/2a$ is lost and the surface regime near $q = \pi/a$ has disappeared. For small wave vectors the elastic transmission remains extremely small, as in the ordered case. This can be explained by the fact that according to Eq. (6) for vanishing wave vectors q the scattered waves do not acquire any phase shift between two scattering events. We therefore expect the scattering matrix of the chain to be independent of the positions of the single scatterers. This argument is no longer true for larger q values, where the transmission depends strongly on the disorder. The strong oscillations of p_{21} for higher q values are strongly sample dependent and can be understood as fingerprints of the specific disorder configuration.

The influence of the disorder on the q dependence of the elastic transmission probability p_{21} for a large sample containing 601 scattering centers is shown in Fig. 4 for the case $\epsilon = 0.1$. The behavior can easily be explained by the fact that perfect constructive or destructive interference of multiply scattered waves is impossible in presence of disorder. Therefore, even if p_{21} remains small in the presence of disorder near $q = 0$, the disorder leads to a strong *relative* increase in the surface regime $0 \leq q \leq 0.18\pi/a$. On the other hand, the transmission is strongly suppressed by the disorder within the transmission window $0.18\pi/a \leq q \leq 0.82\pi/a$. In the other surface regime $0.82\pi/a \leq q \leq \pi/a$ the enhancement factor due

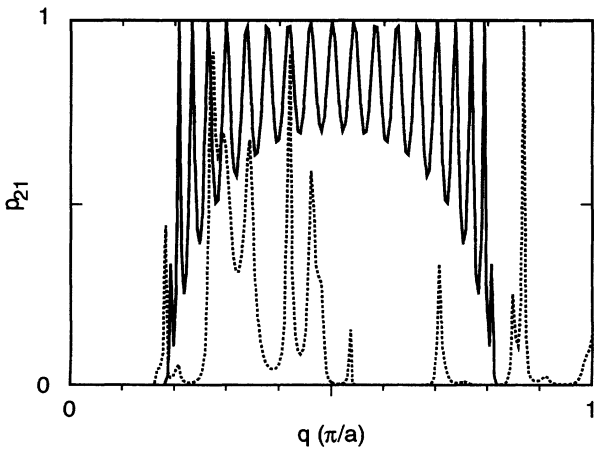

FIG. 3. Elastic transmission probability vs wave vector q for a chain of 20 scatterers without dissipation ($\epsilon = 0.000\,01$), $\delta = 0.7$. Full line, ordered chain; dashed line, disordered chain ($W = 1$).

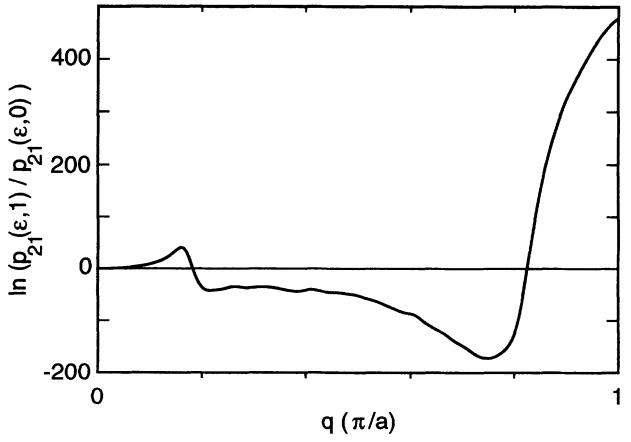

FIG. 4. Ratio of the elastic transmission probabilities of the disordered and of the ordered chain vs wave vector q. The chain length is $N = 601$. The single scatterers are described by the dissipation parameter $\epsilon = 0.1$ and the elastic transmission probability $\delta = 0.7$.

to the disorder is even larger. This enhancement corresponds to the results of Fig. 3, which shows already for a much smaller sample that for strong disorder incoming waves in this q range (e.g., $q = 0.87\pi/a$ in Fig. 3) may traverse the sample with a large probability, so that this regime can no longer be called surface regime.

In Fig. 5 we display the convergence of the dissipation-induced decay length ζ [cf. Eq. (8)] of the elastic transmission probability p_{21} with the chain length N for the wave vector $q = 0.4\pi/a$, which is representative for the bulk regime. We reach satisfactory convergence for $N = 400$. In the surface regime (not shown here) the convergence is even better. The fluctuations in Fig. 5 are related to the $N-1$ peaks of p_{21} for the ordered sample in the q range $0 \leq q \leq \pi/a$ (see, e.g., Fig. 3 for $N = 20$).

The convergence of the disorder-induced decay length ξ [cf. Eq. (9)] of the elastic transmission probability p_{21} is shown in Fig. 6 for the same value of q. We observe strong oscillations which can be seen as fingerprints of the specific disorder in the chain. The convergence in the bulk regime is slower than in Fig. 5, but it is still satisfactory. In the surface regime (not shown here) ξ becomes negative, which corresponds to the strong enhancement of p_{21} in this region (see Fig. 4 and its discussion). For large dissipation ϵ the absolute values of ξ become very large and we shall see below that then they become physically unimportant.

The thus determined asymptotic values of the dissipation-induced decay length ζ and the disorder-induced decay length ξ, as well as the total decay length λ [cf. Eqs. (9)–(11)] are shown in Fig. 7 for both wave-vector regimes: For small dissipation parameter ϵ we have $\lambda \cong \xi$, whereas for large ϵ we find $\lambda \cong \zeta$; i.e., as expected, for small values of ϵ the decay of the elastic transmission probability p_{21} depends strongly on the disorder, whereas for large values of ϵ the decay becomes independent of the disorder. It should be noted that in all cases p_{21} decays

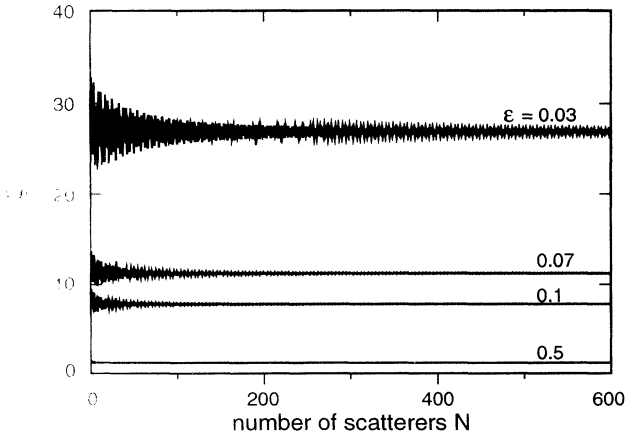

FIG. 5. Convergence of the dissipation-induced decay length ζ (in units of the distance a between adjacent scatterers) for wave vector $q = 0.4\pi/a$. The single scatterers are described the elastic transmission probability $\delta = 0.7$ and different dissipation parameters ϵ.

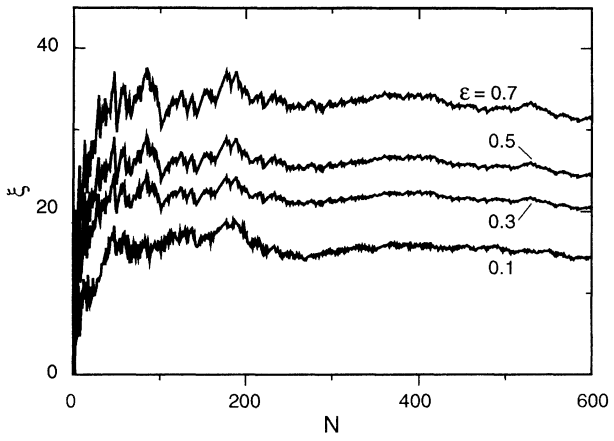

FIG. 6. Convergence of the disorder-induced decay length ξ (in units of the average distance a between adjacent scatterers) for wave vector $q = 0.4\pi/a$. The single scatterers are described the elastic transmission probability $\delta = 0.7$ and different dissipation parameters ϵ.

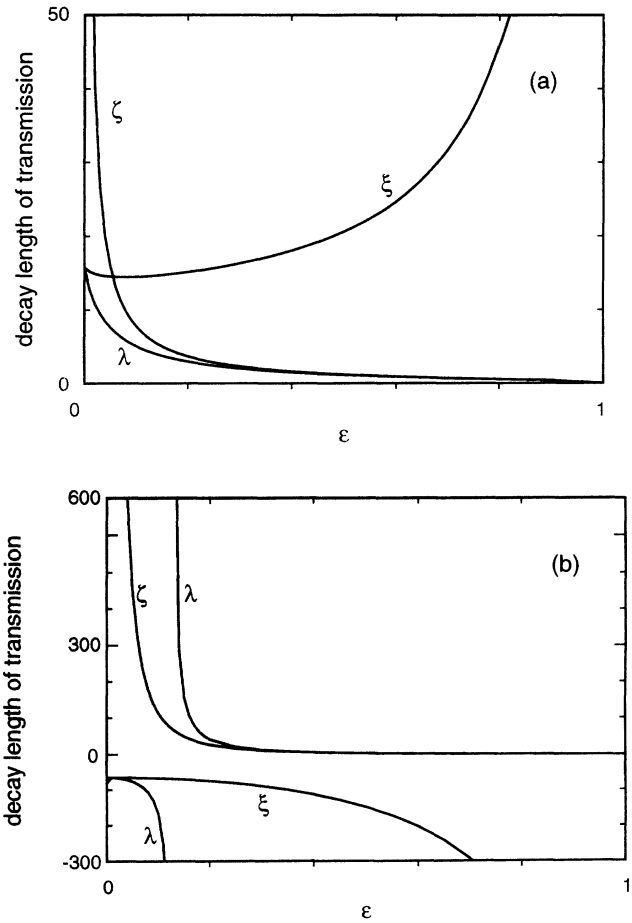

FIG. 7. Dependence of the dissipation-induced decay length ζ, the disorder-induced decay length ξ, and the overall decay length λ on the dissipation parameter ϵ. The results are given for the elastic transmission probability $\delta = 0.7$ of the single scatterers and the wave vectors (a) $q = 0.4\pi/a$ and (b) $q = 0.1\pi/a$.

exponentially with the length of the sample. It can be seen from Fig. 7(b) that the above mentioned large negative ξ values, which are obtained for large dissipation parameters ϵ in the surface regime, do not have a significant influence on the overall decay length λ since, according to Eq. (11), λ is essentially given by the much smaller quantity ζ (the dissipation-induced decay length). Similarly, the negative values of λ for $q \leq 0.12\pi/a$, which can be observed in Fig. 7(b) for small ϵ, are rather insignificant due to the strong exponential decay of the incoming waves which occurs in the surface regime for small dissipation: Here the negative values of λ indicate only the weakening of this strong decay in presence of disorder (see Fig. 3 and the corresponding discussion).

B. Resistance

In the following we shall discuss the influence of the disorder on the resistance. For vanishing dissipation the resistance is essentially given by the inverse of the elastic transmission probability p_{21} [see Eq. (15)]. Accordingly, for an ordered chain the resistance increases exponentially with the chain length in the surface regime, while in the bulk regime it shows oscillations between the minimum value $R = h/e^2$ and some envelope function, which corresponds to the smallest values of p_{21} in this q range; see, e.g., Fig. 3. Since the number of these oscillations increases linearly with the chain length, it follows that the oscillations become very rapid for long chains, in accordance with Fig. 5. These oscillations are somewhat smoothened in presence of disorder (see also Fig. 3).

The influence of the disorder on the q dependence of the resistance is shown in Fig. 8 for a chain of 601 scatterers which is sufficiently long to obtain convergence. For the considered small dissipation parameters ϵ the resistance is again practically determined by the behavior of the elastic transmission probability p_{21}, as shown in Figs. 3 and 4. Thus, the decrease of p_{21} in the bulk regime (see Fig. 4) leads to an increase of the resistance in this q range in presence of disorder, whereas the decrease of the resistance in the surface regimes $0 \leq q \leq 0.18\pi/a$ and $0.82\pi/a \leq q \leq \pi/a$ corresponds to the relative increase of p_{21} in Fig. 4. For increasing dissipation ϵ, interference effects are expected to become less important. This explains the weaker dependence of the resistance on the disorder for larger values of ϵ, which can be inferred from Fig. 8. For $\epsilon = 1$ the resistance becomes completely independent of the disorder and of the wave vector q.

C. Chemical potential

Let us now investigate the influence of the disorder on the chemical potential. For this purpose we have calculated the spatial dependence of the chemical potential. The result for a wave vector q within the bulk regime is shown in Fig. 9 for the ordered and the disordered case. The difference between both cases is rather dramatic:

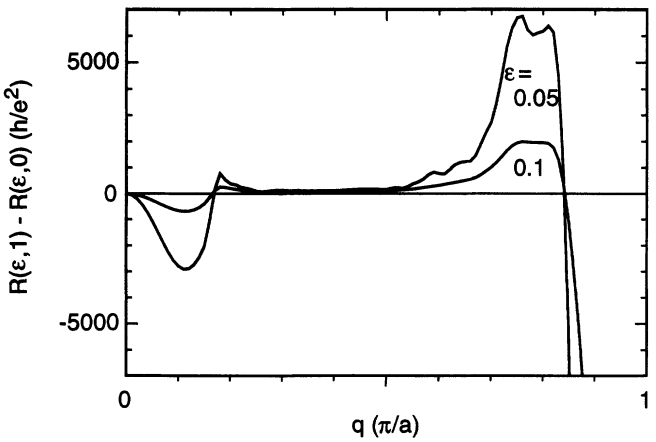

FIG. 8. Difference between the resistances of the disordered $[R(\epsilon,1)]$ and of the ordered chain $[R(\epsilon,0)]$ vs wave vector q. The length of the chains is $N = 601$. The single scatterers are described by the elastic transmission probability $\delta = 0.7$ and the indicated dissipation parameters ϵ.

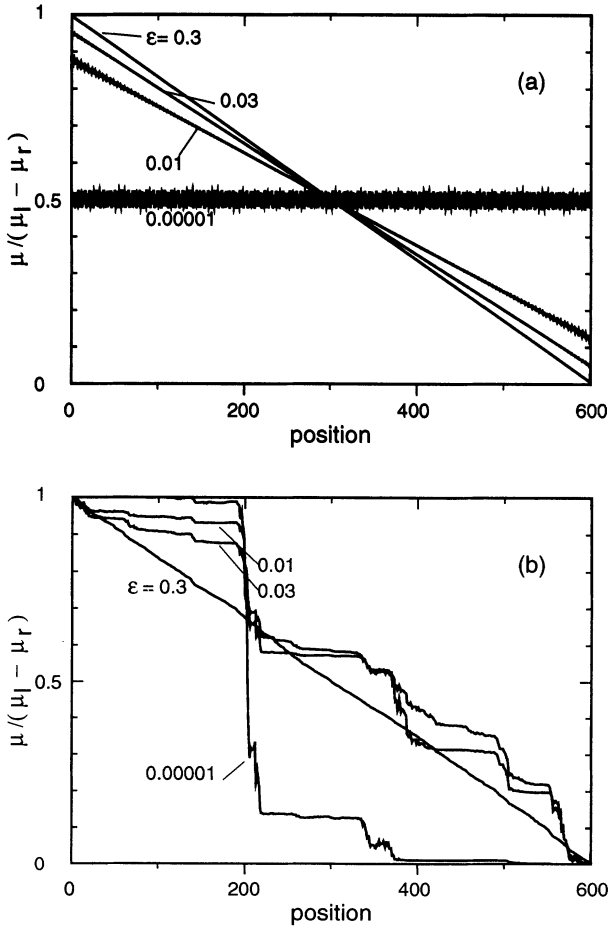

FIG. 9. Chemical potential across the sample for wave vector $q = 0.4\pi/a$. The single scatterers are described by the elastic transmission probability $\delta = 0.7$ and the indicated dissipation parameters ϵ. (a) Ordered chain; (b) disordered chain ($W = 1$).

For the ordered chain in Fig. 9(a) we observe a strongly dissipation-dependent voltage drop at the contacts. The drop is largest for small ϵ values and disappears gradually with increasing dissipation ϵ. Inside the sample, the spatial dependence of the chemical potential remains essentially linear. For extremely small values of ϵ the entire voltage drops at the contacts. Thus, in the limit of vanishing dissipation the chemical potential does not decrease over the sample, but rather displays periodic fluctuations around the mean value $(\mu_l + \mu_r)/2$ which are due to multiple scattering as discussed in Ref. 6.

The situation changes drastically in presence of disorder: In this case [see Fig. 9(b)] we can clearly identify regions of high resistivity inside the sample which lead to rather sharp and large drops in the chemical potential. This behavior can easily be understood if we keep in mind that the fluctuations of the chemical potential are again a consequence of the interference between multiply scattered waves (see also Refs. 6, 19, and 25–27). Obviously there are certain regions in the disordered sample which constitute very large obstacles for the electrons in the transport channel, so that most of the voltage drops at these locations. Between the obstacles the chemical potential remains approximately constant. In the ordered sample the largest obstacles are the contacts, as discussed above.

For the disordered case we have studied in detail the most prominent structure in Fig. 9(b), which occurs around the position $n = 204$. First we confirmed that there is no obvious peculiarity in the sequence of random numbers around this position, i.e., there is no special local arrangement of scatterers, accidentally simulating, e.g., a crystal with a forbidden band for $q = 0.4\pi/a$. [We note in this context that we have chosen the wave vector precisely in such a way that for disorder $W = 1$ even the extreme values $r_n = \pm 1/2$ in Eq. (5) do not yield a phase factor in Eq. (6) with an effective wave vector $q_{\text{eff}} = q(1 + r_n)$ corresponding to the surface regime, so that even a sequence of such extreme random numbers would not yield a "forbidden band" locally.] It is rather the complex multiple scattering in this spatial regime which is responsible for the formation of the obstacle. The relative importance of the obstacle can be changed by altering one of the random numbers near $n = 204$. But unless we alter r_{204}, the chemical potential always drops drastically around $n = 204$. Only by altering r_{204} (which appears to be in no way special otherwise) is it possible to avoid the large drop of the chemical potential in this segment of the chain. The significance of the destructive interference effects between more than just two scatterers becomes obvious by the observation that a change of r_{204} not only diminishes the large decrease at this position, but also the relatively large drops in the neighborhood, namely at $n = 200, 203$, and 205.

As already stated above, a complex interplay between several scatterers leads to the observed drop in Fig. 9(b). We have verified that slight changes of the wave vector $(\pm 0.01\pi/a)$ do not significantly alter this feature, whereas larger changes $(\pm 0.05\pi/a)$ do. Nevertheless, the general behavior of the chemical potential remains similar for all wave vectors q within the bulk regime. However, the spatial location of the voltage drops depends strongly on the wave vector q and on the specific sample. Other ensembles of scatterers (i.e., with other random separations) show a similar striking behavior: there are always several large steps of the chemical potential and nearly flat plateaus in between. In order to corroborate that these are local phenomena, one can divide the chain into several pieces and rearrange them in different order: The steps and plateaus of the chemical potential are rearranged accordingly, unless the steps occur close to a division. In conclusion, there are always some local arrangements of scatterers with a much lower transmission probability than average. Viewing the chain as a series of resistors these specific local arrangements translate into unusually high local resistances. In the hopping description they correspond to chain segments with low hopping probabilities. Both pictures show the same characteristics, namely that the transport is decisively determined by very few exceptionally large obstacles. The high-resistivity regions disappear with increasing dissipation ϵ. For large values of ϵ the spatial distribution of the chemical potential becomes independent of the disorder and we obtain the same linear behavior of the chemical potential as in the ordered case.

In contrast with the above results for the bulk regime, we find for q vectors in the surface regime that the chemical potential μ for vanishing dissipation parameter $\epsilon \to 0$ remains constant in the region near the contacts, i.e., there are "effective contacts" somewhat shifted into the inside of the sample. This shift of the contacts corresponds to the decay length of the incoming waves near the surface in this q range. Beyond the contact region μ drops nearly linearly. The influence of disorder turns out to be negligible in this q range. For increasing dissipation ϵ the shift of the contacts disappears and we obtain again a linear drop of the chemical potential over the full chain length for $\epsilon \to 1$. We note that the transmission probability as well as the conductance can become very (namely exponentially) small in this situation. Nevertheless, there are still some carriers interacting with the local heat baths or reservoirs and therefore we can define still define a chemical potential and derive a conductivity.

D. Conductivity

In the following we discuss the behavior of the conductivity. In the absence of dissipation, the resistance of the chain cannot be characterized by a conductivity, since the resistance does not increase linearly with the length of the chain: in the bulk regime the resistance of ordered chains oscillates with the chain length; for disordered chains as well as in the surface regime (with and without disorder) the resistance increases exponentially with the length of the chain. It follows that the quantity $\sigma(N)$ [Eq. (18)] does not converge to a finite value. In presence of dissipation, however, we may expect that Ohm's law is valid so that the dc transport of sufficiently long chains can be characterized by a conductivity. The conductivities calculated from Eq. (15) are shown in Figs. 10 and 11. Figure 10 displays the convergence of $\sigma(N)$

with the chain length for different degrees of dissipation ϵ. As may be expected, the oscillations of $\sigma(N)$ for ordered samples as well as the fluctuations in disordered samples are damped for large ϵ values and the convergence becomes faster. We obtain satisfactory convergence for chains containing 601 scattering sites for ordered as well as for disordered chains. The comparison of Figs. 9(b) and 10(b) confirms the explanation given above, namely that the sharp drops of the chemical potentials in the disordered case take place in chain segments with high resistivity [corresponding to large drops of the conductivity in Fig. 10(b) near $N = 200$], where incoming waves are strongly backscattered. In the language of the hopping theory, these chain segments would correspond to regions with comparatively small overlap between localized wave functions, and thus with low hopping probability. From this point of view we can understand the localization of the wave functions as an interference effect. In the presence of dissipation the destructive interference of multiply scattered waves in these regions is destroyed and the high-resistivity regions disappear, as seen in Figs. 9(b) and 10(b).

The ϵ dependence of the conductivity is shown in Fig. 11 for different values of q. As expected, for ordered chains the conductivity decreases monotonously with the dissipation parameter ϵ in the bulk regime. The influence of disorder is largest for small ϵ; we obtain a vanishing conductivity in the limit $\epsilon \to 0$. This behavior is directly related to the suppression of the elastic transmission in presence of disorder (see Fig. 4), i.e., to the strong localization of the wave functions. With increasing ϵ the inelastic forward scattering in Eq. (15) becomes more and more important and the dc conductivity is enhanced. In the inelastic limit $\epsilon \to 1$, the interference effects disappear and the conductivity becomes $\sigma = e^2/h$, independent of the disorder and of the wave vector q. The maximum of the $\sigma(\epsilon)$ curve for $q = 0.4\pi/a$ in the presence of disorder can be understood by comparison with the results of Fig. 8, which shows that the effect of disorder is relatively small for this value of q. Accordingly the $\sigma(\epsilon)$ curve for the disordered case approaches the curve for the ordered case already for rather small ϵ values,

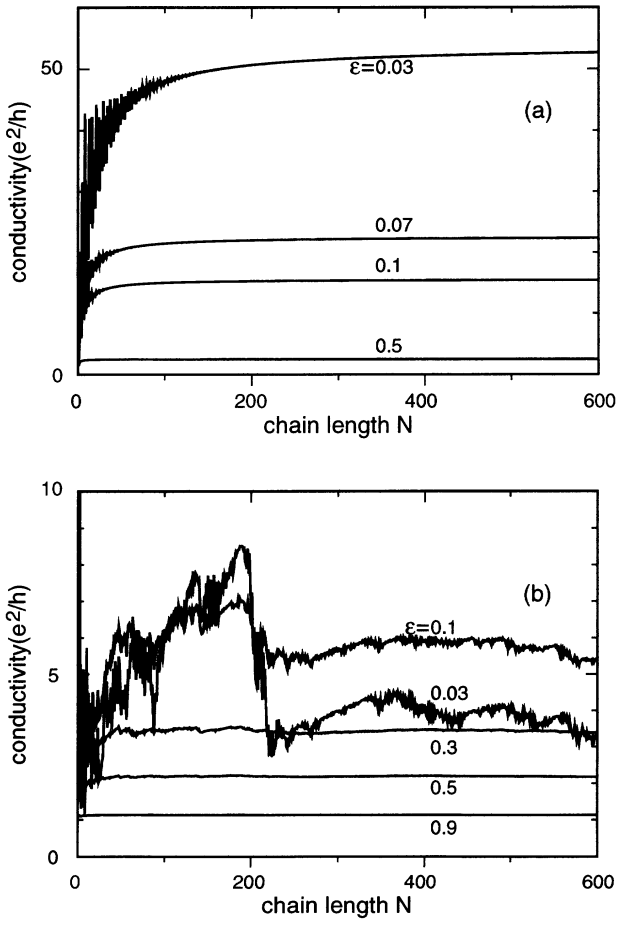

FIG. 10. Convergence of the conductivity for wave vector $q = 0.4\pi/a$. The single scatterers are described the elastic transmission probability $\delta = 0.7$ and the indicated dissipation parameters ϵ. (a) Ordered chain; (b) disordered chain ($W = 1$).

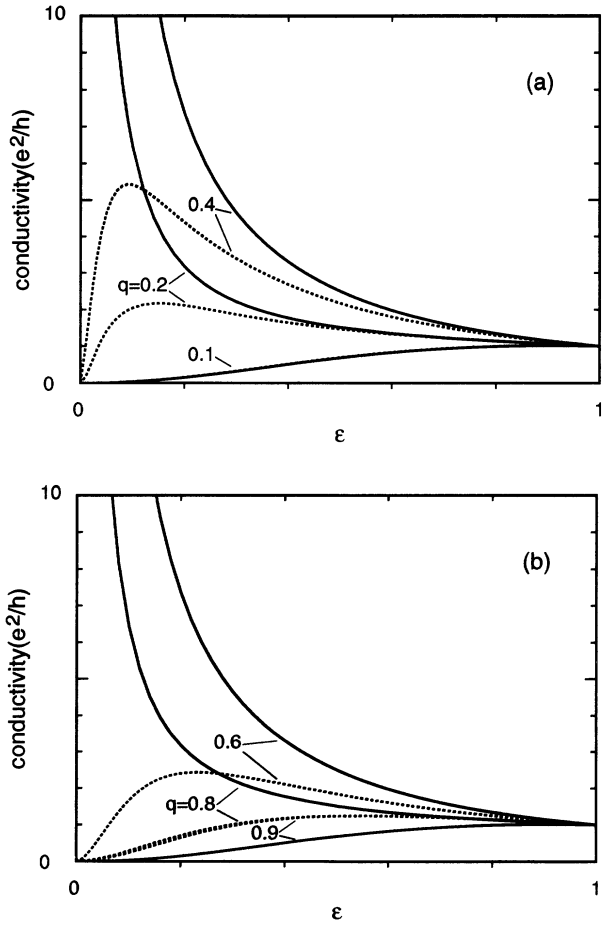

FIG. 11. Dependence of the conductivity on the dissipation parameter ϵ. Full lines, ordered chain; dashed lines, disordered chain ($W = 1$). The results are given for the elastic transmission probability $\delta = 0.7$ of the single scatterers and the wave vectors (a) $q = 0.1, 0.2$, and $0.4\pi/a$ and (b) $q = 0.6, 0.8$, and $0.9\pi/a$.

where the conductivity is still rather large, leading to the prominent maximum at $\epsilon = 0.09$. For $q = 0.2\pi/a$ the behavior is similar, but the maximum is less pronounced since the conductivity of the ordered chain is already small in comparison with the case $q = 0.4\pi/a$. For $q = 0.6\pi/a$ the influence of the disorder is more significant (see Fig. 8) and therefore the conductivity of the disordered chain approaches the curve for the ordered chain (which is identical to the case $q = 0.4\pi/a$) less rapidly. For $q = 0.8\pi/a$ the influence of the disorder is even larger as can be seen from Fig. 8. In consequence, the deviations in Fig. 11 due to the disorder remain significant even for relatively large ϵ. In this case the conductivity increases only slightly above the limiting value e^2/h, leading to a weak maximum around $\epsilon = 0.6$.

In summary, Fig. 11 shows that in the bulk regime the conductivity of disordered samples is always smaller than that of the ordered samples. It increases with the dissipation ϵ up to a wave-vector-dependent maximum. This case is conventionally covered by the hopping picture, in which the conductivity increases with the temperature, i.e., with the inelastic scattering. For larger dissipation the conductivity decreases towards the inelastic disorder-independent limit at $\epsilon = 1$. This is the metallic regime, in which the conductivity decreases with increasing temperature.

In Fig. 11 we have also shown the behavior of $\sigma(\epsilon)$ in the surface regimes. In the case $q = 0.1\pi/a$ the disorder has only negligible influence and the curves for the disordered and the ordered case practically coincide. For $q = 0.9\pi/a$ the conductivity of the disordered chain exceeds significantly that of the ordered chain, in correspondence with the large relative decrease of the resistance in presence of disorder seen in Fig. 8. The agreement between the $\sigma(\epsilon)$ curves for $q = 0.8\pi/a$ and $q = 0.9\pi/a$ is fortuitous. In summary, Fig. 11 shows that in the surface regime the conductivity of disordered samples is always larger than that of ordered systems and it increases monotonously with dissipation towards the q independent limit for $\epsilon = 1$.

IV. CONCLUSIONS

In the present paper we have investigated the influence of dissipation on the dc transport properties of a disordered chain by using the Landauer-Büttiker approach. We have shown that within this approach the localization of electronic states in presence of disorder can be understood as a consequence of the destructive interference of multiply scattered waves. We have demonstrated for small dissipation that, depending on the particular disordered configuration of the scatterers in the sample, the chemical potential along the chain features characteristic steps and intermediate plateaus. These correspond to chain segments of destructive and of constructive interference, respectively. It turned out that there is usually one highly resistive segment which dominates the behavior of the entire chain. This gives rise to the observed dramatic changes of the chemical potential for certain arrangements of the scatterers.

In the absence of dissipation the localization due to the disorder leads to vanishing conductance. We have demonstrated that the onset of conductance for small dissipation, which is commonly described within the hopping theory, can be explained by the fact that destructive interference effects are gradually suppressed with increasing dissipation due to the loss of phase memory. This description thus leads to an alternative physical understanding instead of the usually employed hopping picture, which expresses the conductivity in terms of transition rates between localized states at finite temperature. It should be noted that our usage of the Landauer-Büttiker approach has several advantages with respect to the hopping model: In particular, the present approach remains valid over the full range of dissipative coupling parameters, the presented description of the dc transport with and without dissipation is conceptually the same, and it describes equally well the ordered chain. In other words, the Landauer-Büttiker picture can be considered as a general approach which, in principle, covers the full range of dc properties, without any restriction, e.g., to low temperatures.

However, to make the description complete, one should relate the scattering parameters more closely to the underlying physical interactions. In particular, the elastic part of the scattering matrices can be easily related to a Hamiltonian, such as, e.g., the Anderson Hamiltonian. This immediately introduces a q dependence of the scattering parameters. Work along these lines is in progress.[20] Moreover, as mentioned in the Introduction, it is possible to describe the dissipation in terms of the interaction between electrons and lattice vibrations by introducing a heat bath of harmonic oscillators (see, e.g., Ref. 14). This not only yields a microscopic derivation of the dissipation parameter ϵ, but also allows us to establish its temperature dependence. It would also be interesting to generalize the present one-dimensional chain model to wider systems in which more than one transport channel connects the left and the right contact. In this way the description of two-dimensional and three-dimensional transport should be feasible. A systematic approach for the calculation of an appropriate scattering matrix for such multiply connected systems has been given in Ref. 28. Another interesting extension is the consideration of electron-electron interaction as discussed recently.[29]

[1] See, e.g., N. F. Mott and E. A. Davis, *Electronic Processes in Non-Crystalline Materials* (Oxford University Press, Clarington, 1979).

[2] R. Landauer, IBM J. Res. Dev. **1**, 223 (1957); Philos. Mag. **21**, 863 (1970); Phys. Lett. **85A**, 91 (1981).

[3] A. MacKinnon and B. Kramer, Z. Phys. B **53**, 1 (1981); B. Kramer and M. Schreiber, in *Fluctuations and Stochastic Phenomena in Condensed Matter*, edited by L. Garrido, Lecture Notes in Physics Vol. 268 (Springer, Berlin, 1987), p. 351.

[4] M. Büttiker, Phys. Rev. B **32**, 1846 (1985); **33**, 3020 (1986).
[5] K. Maschke and M. Schreiber, Phys. Rev. B **44**, 3835 (1991).
[6] M. Schreiber and K. Maschke, Z. Phys. B **85**, 123 (1991).
[7] D. Lenstra and R. T. M. Smokers, Phys. Rev. B **38**, 6452 (1988).
[8] Y. B. Band, H. U. Baranger, and Y. Avishai, Phys. Rev. B **45**, 1488 (1992).
[9] A. N. Khondker and M. A. Alam, Phys. Rev. B **44**, 5444 (1991).
[10] J. L. D'Amato and H. M. Pastawski, Phys. Rev. B **41**, 7411 (1990).
[11] M. Schreiber and K. Maschke, Philos. Mag. B **65**, 639 (1992); in *Photonic Band Gaps and Localization,* edited by C. M. Soukoulis (Plenum, New York, 1993), p. 439.
[12] P. A. Schulz, D. S. Galvão, and M. J. Caldas, Phys. Rev. B **44**, 6073 (1991).
[13] A. S. Sen and S. Gangopadhyay, Physica A **186**, 270 (1992).
[14] S. Datta, J. Phys. Condens. Matter **2**, 8023 (1990).
[15] R. Landauer, Phys. Scr. **T42**, 110 (1992).
[16] R. Landauer, J. Phys. Condens. Matter **1**, 8099 (1989).
[17] H. L. Engquist and P. W. Anderson, Phys. Rev. B **24**, 1151 (1981).
[18] M. Y. Azbel, Phys. Rev. B **47**, 15 688 (1993).
[19] G. Burmeister, K. Maschke, and M. Schreiber, Phys. Rev. B **47**, 7095 (1993).
[20] R. Hey, M. Schreiber, and K. Maschke (unpublished).
[21] S. Datta, Phys. Rev. B **45**, 1347 (1992).
[22] S. Datta and M. P. Anantram, Phys. Rev. B **45**, 13 761 (1992).
[23] F. Hecking and Y. V. Nazarov, Phys. Rev. B **44**, 9110 (1991).
[24] Z. Chen and R. S. Sorbello, Phys. Rev. B **44**, 12 857 (1991).
[25] M. Büttiker, Phys. Rev. B **40**, 3409 (1989).
[26] M. Büttiker, IBM J. Res. Dev. **32**, 63 (1988).
[27] M. Büttiker, in *Analogies in Optics and Micro-Electronics*, edited by W. van Haeringen and D. Lenstra (Kluwer Academic, Dordrecht, 1990), p. 185.
[28] F. Gagel and K. Maschke (unpublished).
[29] Y. Meir and N. S. Wingreen, Phys. Rev. Lett. **68**, 2512 (1992).